

# Preparation and phase transition characterization of VO<sub>2</sub> thin film on single crystal Si (100) substrate by sol–gel process

Qiwu Shi · Wanxia Huang · Jiazhen Yan ·  
Yubo Zhang · Mao Mao · Yang Zhang ·  
Yuanjie Xu · Yaxin Zhang

Received: 26 March 2011 / Accepted: 28 June 2011 / Published online: 6 July 2011  
© Springer Science+Business Media, LLC 2011

**Abstract** Vanadium dioxide (VO<sub>2</sub>) thin films were fabricated on single crystal Si (100) substrates by sol–gel method, including a process of annealing a vanadium pentoxide (V<sub>2</sub>O<sub>5</sub>) gel precursor at different temperatures. The crystalline structure and morphology of the films were investigated by XRD, FE-SEM and AFM, indicating that the films underwent the grain growth, agglomeration and grain refinement process with increased annealing temperatures. The film annealed at 500 °C exhibits the formation of VO<sub>2</sub> phase with a strong (011) preferred orientation and high crystallinity, the surface of the film is uniform and compact with a grain size of about 120 nm. Meanwhile, the film exhibits excellent phase transition properties, with a decrease of transmittance from 35.5 to 2.5% at  $\lambda = 25 \mu\text{m}$  and more than 3 orders of resistivity magnitude variation below and above the phase transition temperature. The phase transition temperature is evaluated at 60.4 °C in the heating transition and 55.8 °C in the cooling transition. Furthermore, the phase transition property of the VO<sub>2</sub> film appears to be able to remain stable over repetitive cycles 100 times.

**Keywords** VO<sub>2</sub> thin film · Sol–gel · Single crystal Si substrate · Phase transition

Q. Shi · W. Huang (✉) · J. Yan · Y. Zhang · M. Mao ·  
Y. Zhang · Y. Xu  
College of Materials Science and Engineering,  
Sichuan University, Chengdu 610064, Sichuan,  
People's Republic of China  
e-mail: huangwanxiascu@yahoo.com.cn

Y. Zhang  
School of Physical Electronics, University of Electronic  
Science and Technology of China, Chengdu 610054,  
Sichuan, People's Republic of China

## 1 Introduction

Vanadium dioxide (VO<sub>2</sub>) is a transition-metal oxide that undergoes a reversible first order phase transition from a low temperature semiconductor phase to a high temperature metal phase nearly 68 °C, which can be manipulated by doping or stress [1, 2]. The transition is accompanied by significant and abrupt change in optical and electrical properties [3, 4]. Recently, it has been observed that this phase transition can be triggered by not only temperature, but also electric field, light and pressure [5–7]. All these properties make VO<sub>2</sub> as a candidate material for a variety of applications, such as thermochromic windows, IR uncooled bolometer, optical switching, and sensor devices [8–11]. Wherein, the electric field triggered phase transition in VO<sub>2</sub> is particularly suitable for applications as electrical switching, modulator and memory devices [12, 13].

Single crystal Si is one of the most frequently used substrates in VO<sub>2</sub>-based devices due to its well-known electrical properties and low price. Moreover, the high-purity Si has been demonstrated to be not only the most transparent but also the least dispersive medium in the terahertz region, and hence is especially applicable as substrate contacts in VO<sub>2</sub>-based THz devices [14, 15]. Several methods including pulse laser deposition, reactive sputtering, chemical vapor deposition and sol–gel method have been used to deposit VO<sub>2</sub> films. Of these methods, the sol–gel process is regarded as a quite promising and important method because of its low cost, easy coating of large-scale surface, flexible control of film thickness, and many other advantages [16–18]. However, it is usually difficult to obtain a good film of VO<sub>2</sub> on Si substrate by sol–gel process, for their bad contact performance induced by the lack of hydrophilic nature of Si interface.

In this research, we described the fabrication of VO<sub>2</sub> films on crystalline Si substrate using a sol–gel method

followed by an annealing process at different temperatures. The Si substrate was pre-treated with hydrophilic solution and obtained an improved hydrophilicity, which resulted in a better contact performance between the film and Si substrate. The crystalline structure and morphology of the films were studied using X-ray diffraction (XRD), field emission scanning electron microscopy (FE-SEM) and atomic force microscopy (AFM). Moreover, the phase transition properties were investigated using an FT-IR method and a resistivity measurement system.

## 2 Experiments

### 2.1 Surface cleaning and hydrophilic treatment of Silicon substrate

In a surface treatment, the n-type single crystal Si (100) substrate ( $\sim 2000 \Omega \text{ cm}$  resistivity, Hefei Kejing Materials Technology Co., Ltd., China) was first pre-treated by ultrasonic cleaning in ethyl alcohol for 30 min and rinsing with de-ionized (DI) water for 5 min, in order to remove some organic contaminations on the surface. And then a thin  $\text{SiO}_x$  layer was formed by oxidizing the Si substrate in the hydrophilic solution composed of mixture of concentrated  $\text{H}_2\text{SO}_4$  and  $\text{H}_2\text{O}_2$  with a ratio of 1:1 at  $90^\circ\text{C}$  for 120 min. Through the treatment, the Si surface underwent surface functionalization through hydroxylation [19]. The cation impurities could be also removed in this treatment. After these treatments, the substrate was rinsed again with DI water for 5 min, and blown dry at  $60^\circ\text{C}$  for 15 min.

### 2.2 Sample preparation

We prepared  $\text{V}_2\text{O}_5$  sol with a method described in the previous paper [20], in which the melting  $\text{V}_2\text{O}_5$  underwent hydrolysis and polycondensation reaction to form a colloid. The sol then evolved toward the formation of inorganic network (gel) [21]. According to Ref. [22], the  $\text{V}_2\text{O}_5$  gels obtained a structure as described in Fig. 1. Following by

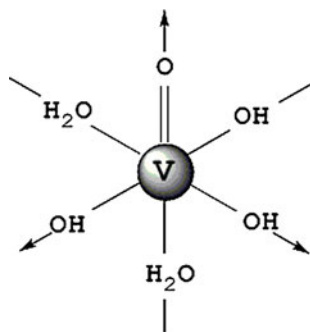


**Fig. 1** Structure representation of the  $\text{V}_2\text{O}_5$  gel

water adsorption and dissociation occurs at the oxide–water interface leading to the acid dissociation of  $\text{V}-\text{OH}$  groups, the  $\text{V}_2\text{O}_5$  gels could then be described as polyvanadic acids  $\text{H}_x\text{V}_2\text{O}_5$ . We proved this model in a later subsection.

The precursor films were deposited on Si (100) substrate by dip coating method. Then the films were dried around  $90^\circ\text{C}$  for 15 min to remove the residual moisture. The dip coating process was repeated to increase the film thickness. The binding of  $\text{V}_2\text{O}_5$  gel with Si substrate includes two approaches: a direct adsorption and a chemical linker, which was similar to the phenomena reported in Ref. [23]. The chemical linker provided a nearly covalent-strength bond between the gel and the surface due to the hydroxylation of Si interface.

In order to form the  $\text{VO}_2$  films, subsequent annealing was done in a furnace at the temperatures of 110, 300, 500 and  $700^\circ\text{C}$  for 1.5 h in a static atmosphere of nitrogen, with a heating rate of  $8^\circ\text{C min}^{-1}$ . The resulting films with a thickness of about 150 nm were obtained after cooling down from the annealing temperature.

### 2.3 Characterizations

Contact angles with DI water were performed by a pendant-drop method with an automatic contact angle analyzer combined with a flash camera equipment (DSA 100, Kruss, Germany) at room temperature. The reported measurements are averages of five contact angle measurements recorded on each sample.

Functional groups of the  $\text{V}_2\text{O}_5$  gel were analyzed by FT-IR spectrometer (Tensor 27, Bruker, Germany) to confirm the existence of  $-\text{OH}$  groups. The resolution of detection was set as  $4 \text{ cm}^{-1}$ . The sample was acquired by spreading the gel on KBr plates, and then measured after different roasting time at  $110^\circ\text{C}$ .

Crystalline structure of the films was determined by XRD (X' Pert, Philips) with  $\text{Cu K}\alpha$  ( $\lambda = 0.15406 \text{ nm}$ ) radiation source.

Surface morphology was studied by FE-SEM (Inspect F, FEI, Holland) with an accelerating voltage of 20 kV. The magnifying power was 80 000x. The morphology was also investigated by AFM (Nanoscope Multimode APM, Veeco Instrument, America) with a tapping mode under ambient conditions. Etched Si nanoprobe tip with spring constant of  $40 \text{ N m}^{-1}$  was used.

Optical properties of the films were investigated by FT-IR spectrometer to analyze the transmittance of the films at the middle infrared range below and above the  $\text{VO}_2$  phase transition temperature.

Electrical resistivity dependent on the temperature was measured by the conventional four-point probe method combined with a heater element.

### 3 Results and discussion

#### 3.1 Contact angles

The Si substrate with no hydrophilic treatment has bad hydrophilicity and the contact angle is about  $68.0^\circ$  ( $t = 0$  min). With the oxidization of the Si surface, the contact angle decreased obviously and showed a value of  $12.1^\circ$  after a 120 min oxidizing treatment, indicating a significant enhanced hydrophilicity. It was attributed to the increased compactness of  $\text{SiO}_2$  layer, followed by a combination of  $-\text{OH}$  groups on the substrate surface. The  $\text{Si}-\text{OH}$  groups increase the surface energy and then improve the hydrophilicity of Si surface.

#### 3.2 FT-IR spectrum of $\text{V}_2\text{O}_5$ gel

The  $\text{V}_2\text{O}_5$  gel is an inorganic network derived from hydrolysis and polycondensation reaction of melting  $\text{V}_2\text{O}_5$  in DI water. Figure 2 shows the FT-IR spectra of the gel on KBr plates in the spectral range  $4,000\text{--}400\text{ cm}^{-1}$ . A broad peak below  $850\text{ cm}^{-1}$  could be assigned to characteristic distribution of  $\text{V}-\text{O}$  groups. Moreover, two strong peaks at  $3,460$  and  $1,639\text{ cm}^{-1}$  correspond to stretching vibration and bending vibration bands of  $-\text{OH}$  groups respectively, which could be assigned to water absorption or due to chemical bonding of  $-\text{OH}$  groups in the  $\text{V}_2\text{O}_5$  gel. The intensity of these two peaks versus the roasting time at  $110^\circ\text{C}$  shows a tendency of reduction, denoting a consumption of  $-\text{OH}$  groups with roasting. However, the two peaks still exist after roasting 10 min indicating a chemical bonding of  $-\text{OH}$  groups.

Furthermore, we tested the PH of the  $\text{V}_2\text{O}_5$  gel, and observed a value in the range of  $0.5\text{--}1.0$ , which means a strong acid. It could be explained by the acid dissociation

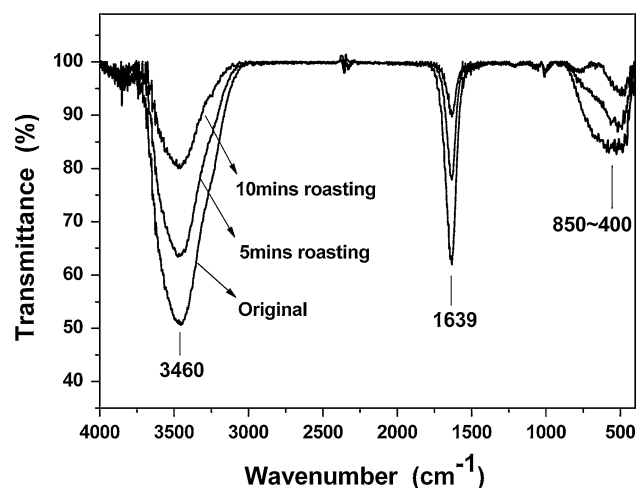
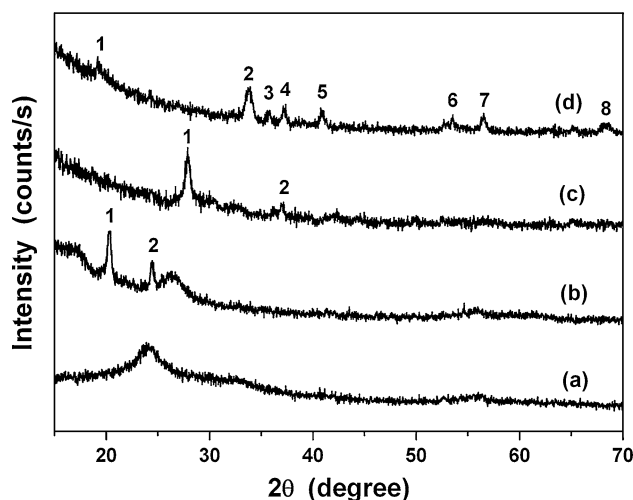


**Fig. 2** FTIR spectrum of the  $\text{V}_2\text{O}_5$  gel on KBr plates after different roasting time at  $110^\circ\text{C}$

of  $\text{V}-\text{OH}$  groups in the gel system. All these results confirm the gel structure existing in the form of polyvanadic acids  $\text{H}_x\text{V}_2\text{O}_5$  as described in Fig. 1.

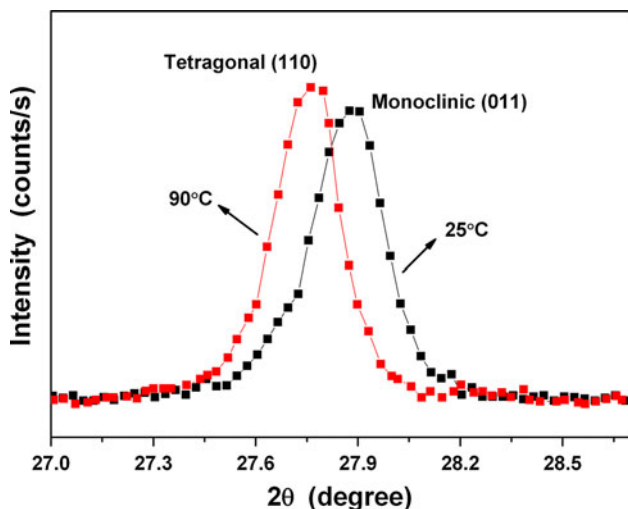
#### 3.3 XRD

Figure 3 shows XRD patterns of  $\text{VO}_x$  films annealed at various temperatures. As seen in Fig. 3a, only one broad peak extending from  $20^\circ$  to  $27^\circ$  is observed for the sample annealed at  $110^\circ\text{C}$ . It means the film is still amorphous. The XRD pattern of the film annealed at  $300^\circ\text{C}$  indicates amorphous characteristics (Fig. 3b), but peaks  $1(2\theta = 20.30^\circ)$  and  $2(2\theta = 24.44^\circ)$  are shown, due to diffractions from (001) planes of  $\text{V}_2\text{O}_5$  and (210) planes of  $\text{V}_4\text{O}_9$  phases, respectively. When the film was annealed at  $500^\circ\text{C}$ , Fig. 3c shows peaks  $1(2\theta = 27.86^\circ)$  and  $2(2\theta = 37.14^\circ)$  that are related to (011) and (200) planes of  $\text{VO}_2$  phase respectively. No other vanadium oxides are detected. In addition, the (011) peak is strong, but the (200) peak is weak. It indicates that the film has a strong orientation relation to the Si substrate, which may be either due to the lattice match between the film and the substrate [24]. The full width at half maximum (FWHM) of the (011) peak is narrow with a value of  $0.42$ , implying high crystallinity of the film. The number of the observed peaks for the film annealed at  $700^\circ\text{C}$  increases. Figure 3d shows peaks  $1(2\theta = 19.15^\circ)$ ,  $2(2\theta = 33.89^\circ)$ ,  $3(2\theta = 35.74^\circ)$ ,  $4(2\theta = 37.24^\circ)$ ,  $5(2\theta = 40.76^\circ)$ ,  $6(2\theta = 53.54^\circ)$ ,  $7(2\theta = 56.51^\circ)$  and  $8(2\theta = 68.57^\circ)$ , which may coincide with the diffractions from (200) planes of  $\text{V}_3\text{O}_5$ ,  $(\bar{3}11)$  planes of  $\text{VO}_2$ , (311) planes of  $\text{V}_6\text{O}_{13}$ , (200) planes of  $\text{VO}_2$ ,  $(\bar{4}11)$  planes of  $\text{V}_3\text{O}_5$ , (221) and (222) planes of  $\text{V}_6\text{O}_{13}$  and (611) planes of  $\text{VO}_2$  phases, respectively. The variation in the XRD patterns is resulted from differences in the crystallinity of the films annealed at different temperatures.



**Fig. 3** XRD patterns of the  $\text{VO}_2$  films annealed at (a)  $110^\circ\text{C}$ , (b)  $300^\circ\text{C}$ , (c)  $500^\circ\text{C}$  and (d)  $700^\circ\text{C}$

Furthermore, concerning the phase transition of the  $\text{VO}_2$  films illustrated in this work, the changes in temperature-controlled XRD patterns of the film annealed at  $500^\circ\text{C}$  was shown in Fig. 4. The diffraction peak at  $2\theta = 27.86^\circ$



**Fig. 4** Temperature-controlled XRD patterns of the film annealed at  $500^\circ\text{C}$ , taken at  $25^\circ\text{C}$  and  $90^\circ\text{C}$

corresponds to the (011) planes of monoclinic  $\text{VO}_2$  (taken at room temperature about  $25^\circ\text{C}$ ). But the peak shifts to a lower angle of  $2\theta = 27.75^\circ$  (taken at  $90^\circ\text{C}$  above the phase transition temperature), with a tiny increase of the diffraction intensity. It is attributed to the changes of the film from monoclinic to tetragonal phase transition, which has been also illustrated in our previous paper [25].

### 3.4 FE-SEM and AFM

The morphology and microstructure of the films were further investigated by FE-SEM and AFM. Figure 5 shows the FE-SEM photographs for the films annealed at different temperatures. The film annealed at  $110^\circ\text{C}$  (Fig. 5a) shows a flat surface. According to the former XRD results, we assume that the film was formed by the dry  $\text{V}_2\text{O}_5$  gel film without crystallizing. Figure 5b exhibits the similar morphology, while extremely weak particles are formed at this annealing temperature ( $300^\circ\text{C}$ ). Increasing annealing temperature at  $500^\circ\text{C}$  resulted in more clear grain boundaries and grain growth. It is seen in the Fig. 5c that the surface of  $\text{VO}_2$  film is uniform and compact with a grain size of about  $120\text{ nm}$ . There are no obvious surface defects observed in

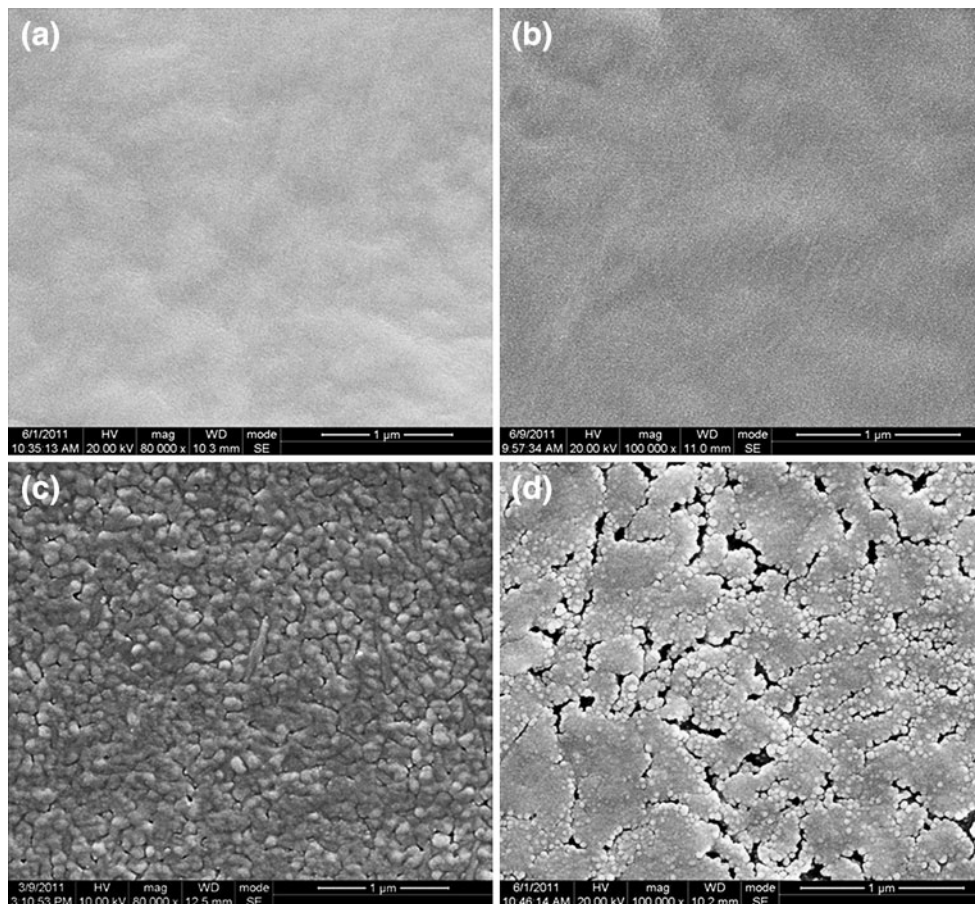


**Fig. 5** SEM images of the  $\text{VO}_2$  films annealed at (a)  $110^\circ\text{C}$ , (b)  $300^\circ\text{C}$ , (c)  $500^\circ\text{C}$  and (d)  $700^\circ\text{C}$

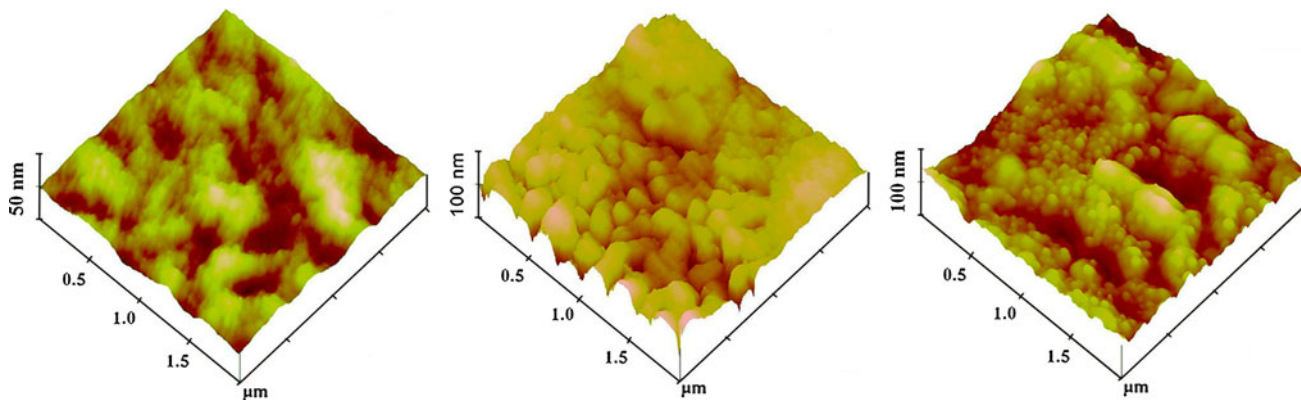


**Fig. 6** AFM images of the VO<sub>2</sub> films annealed at (a) 300 °C, (b) 500 °C and (c) 700 °C

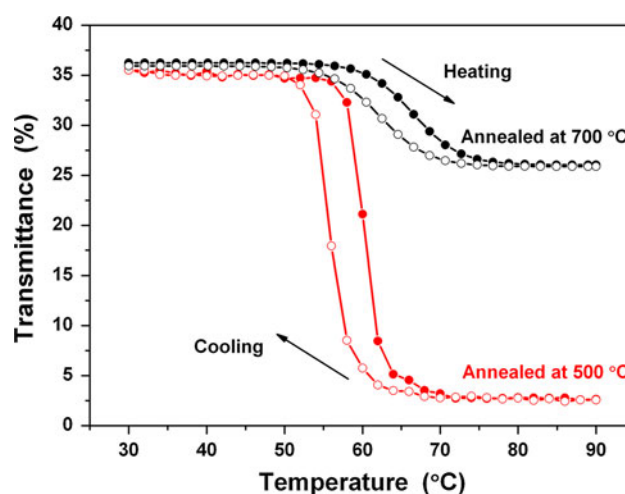
the image, which may be formed during the dip coating and drying process. But the film annealed at 700 °C shows obvious microcracks, due to the pronounced grain refinement. The microcracks are harmful for the phase transition properties of VO<sub>2</sub> films [26].

AFM image (Fig. 6) shows the area of 2 μm × 2 μm morphologies of the films annealed at 300, 500 and 700 °C. It suggests that the films underwent the grain growth, agglomeration and grain refinement process with increased annealing temperatures, as illustrated by FE-SEM photographs.

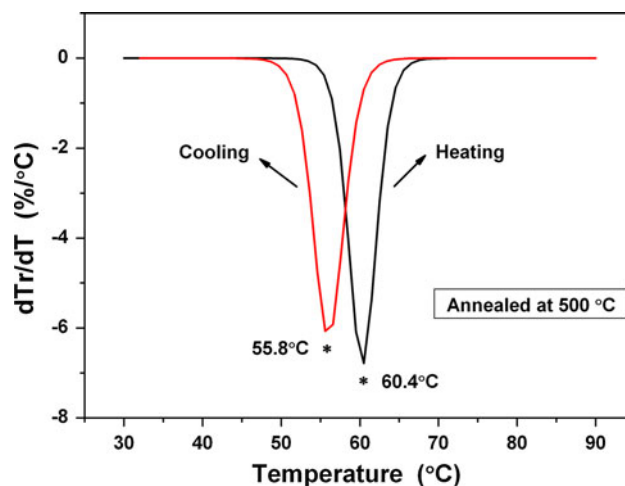
### 3.5 FT-IR in VO<sub>2</sub> thin films

Figure 7 shows a graph of transmittance against temperature at λ = 25 μm, the wavelength at which the sharpest contrast was observed below and above the phase transition temperature. The films annealed at 110 and 300 °C did not show any phase transition properties during the detecting temperature range from 30 to 90 °C, for there is no VO<sub>2</sub> phase existed. The transmittance for the film annealed at 700 °C decreases from 36.2 to 25.8% during the phase transition. The low variation could be attributed to the multiphase coexistence and the obvious microcracks. However, for the film annealed at 500 °C, the curve exhibits a decrease of transmittance from 35.5 to 2.5%. Moreover, as the derivative of the temperature dependence of transmittance (dTr/dT) (Fig. 8), the phase transition temperature of the film annealed at 500 °C could be evaluated to be 60.4 °C in the heating transition and 55.8 °C in the cooling transition. The significant decrease in transition temperature and hysteresis width of VO<sub>2</sub> film on Si has been attributed to either the compressive strain along [011] direction [27], or larger fraction of +4 valence vanadium [28].

As for the cycle stability, the repeated phase transition with 30, 50 and 100 times and the accompanied optical changes of the VO<sub>2</sub> film annealed at 500 °C were



**Fig. 7** Hysteresis curves of transmittance against temperature at 25 μm for the VO<sub>2</sub> films annealed at (a) 500 °C and (b) 700 °C



**Fig. 8** Transition temperature of the VO<sub>2</sub> film annealed at 500 °C, determined during temperature ramping up and ramping down, respectively

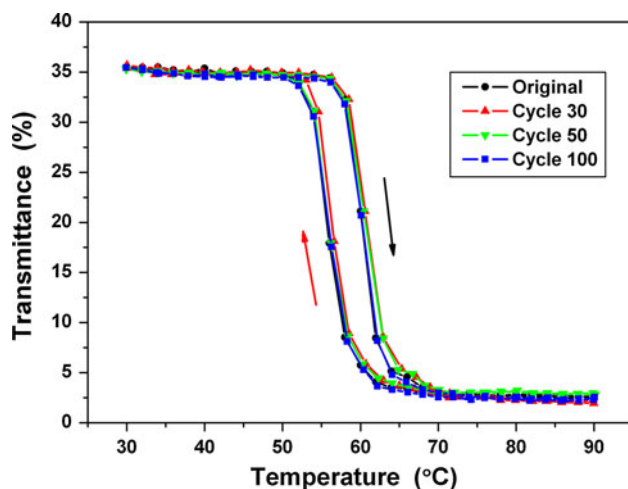


**Fig. 9** Hysteresis curves of transmittance against temperature obtained for 30, 50 and 100 cycles in the VO<sub>2</sub> film annealed at 500 °C

measured, shown in Fig. 9. The hysteresis curves of transmittance against temperature suggest that the thermal triggered change of transmittance at  $\lambda = 25 \mu\text{m}$  can revert back to its original value over a large number of cycles without deviations of the critical transition temperatures and hysteresis widths. The phase transition property of the VO<sub>2</sub> films appears to be able to remain stable during repetitive cycles. They would therefore be convenient for the variety of applications discussed earlier.

### 3.6 Resistivity

The electrical phase transition property of VO<sub>2</sub> film annealed at 500 °C and 700 °C were studied by the four-point probe method to record variations in resistivity with temperature (Fig. 10). A typical hysteresis cycle, similar to that of the FT-IR curves, was also observed. For the film annealed at 700 °C, the resistivity of the film drops from 14.9  $\Omega \text{ cm}$  at 25 °C to 0.52  $\Omega \text{ cm}$  above 75 °C. By contrast, the resistivity of the film annealed at 500 °C has an abrupt drop from 11.6  $\Omega \text{ cm}$  at 25 °C to 0.01  $\Omega \text{ cm}$  above 75 °C. The resistivity of the VO<sub>2</sub> film changes by more than 3 orders of magnitude when cycled through the phase transition. This amplitude of variation is also larger than the usually obtained change of 2–3 orders of VO<sub>2</sub> films.

## 4 Conclusions

In summary, we fabricated VO<sub>2</sub> thin films on single crystal Si (100) substrates by sol–gel method, including a process of annealing a vanadium pentoxide (V<sub>2</sub>O<sub>5</sub>) gel precursor at 110, 300, 500 and 700 °C. The Si substrate was pre-treated

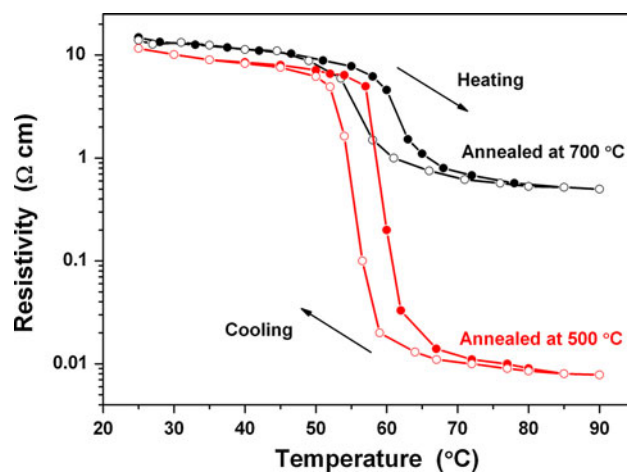


**Fig. 10** Hysteresis curves of resistivity against temperature of the VO<sub>2</sub> films annealed at (a) 500 °C and (b) 700 °C

with hydrophilic solution and obtained an improved hydrophilicity. A decrease of contact angle from 68.0° to 12.1° resulted in a better contact performance between the film and Si substrate.

The film annealed at 110 °C is still amorphous, but the films underwent the grain growth, agglomeration and grain refinement process with increased annealing temperatures. The film annealed at 500 °C exhibits the formation of VO<sub>2</sub> phase with a strong (011) preferred orientation and high crystallinity, the surface of the film is uniform and compact with a grain size of about 120 nm. Meanwhile, the films annealed at 110 and 300 °C did not show any phase transition properties during the detecting temperature range from 30 to 90 °C, for there is no VO<sub>2</sub> phase existed. The transmittance for the film annealed at 700 °C decreases from 36.2 to 25.8% at  $\lambda = 25 \mu\text{m}$  during the phase transition. But the film annealed at 500 °C exhibits excellent phase transition properties, with a decrease of transmittance from 35.5% to 2.5% and more than 3 orders of resistivity magnitude variation below and above the phase transition temperature. The phase transition temperature is evaluated at 60.4 °C in the heating transition and 55.8 °C in the cooling transition. Furthermore, the phase transition property of the VO<sub>2</sub> film appears to be able to remain stable over repetitive cycles 100 times. These results indicate that the sol–gel method could be a suitable process for fabricating VO<sub>2</sub> film with excellent phase transition properties on Si substrate.

**Acknowledgments** This work was financially supported by the National Science Foundation of China (Grant Nos. 61072036) and the Science and Technology Supporting Programs Fund Project of Sichuan province (2009SZ0199). We would also thank Analytical and Testing center of Sichuan University for their XRD analysis.

## References

- Manning TD, Parkin IP, Pemble ME, Sheel D, Vernardou D (2006) Intelligent window coatings: atmospheric pressure chemical vapor deposition of tungsten-doped vanadium dioxide. *Chem Mater* 16:744–749
- Muraoka Y, Ueda Y, Hiroi Z (2002) Large modification of the metal-insulator transition temperature in strained VO<sub>2</sub> films grown on TiO<sub>2</sub> substrates. *J Phys Chem Solids* 63:965–967
- Lappalainen J, Heinilehto S, Jantunen H, Lantto V (2008) Electrical and optical properties of metal-insulator-transition VO<sub>2</sub> thin films. *J Electroceram* 22(1–3):73–77
- Morin FJ (1959) Oxides which show a metal-insulator transition at the neel temperature. *Phys Rev Lett* 3:34–36
- Kim HT, Chae BG, Youn DH, Kim G, Kang KY, Lee SJ, Kim K, Lim YS (2005) Raman study of electric-field-induced first-order metal-insulator transition in VO<sub>2</sub>-based devices. *Appl Phys Lett* 86:242101
- Cavalleri A, Tóth Cs, Siders CW, Squier JA et al (2001) Femtosecond structure dynamics in VO<sub>2</sub> during an ultrafast solid–solid phase transition. *Phys Rev Lett* 87:237401
- Cao J, Ertekin E, Srinivasan V, Fan W, Huang S et al (2009) Strain engineering and one-dimensional organization of metal-insulator domains in single-crystal vanadium dioxide beams. *Nat Nanotechnol* 4:732–737
- Manning TD, Parkin IP (2004) Atmospheric pressure chemical vapour deposition of tungsten doped vanadium (IV) oxide from VOCl<sub>3</sub>, water and WCl<sub>6</sub>. *J Mater Chem* 14:2554–2559
- Jerominek H, Picard F, Vincent D (1993) Vanadium oxide films for optical switching and detection. *Opt Eng* 32:2092–2099
- Huang WX, Yin XG, Huang CP, Wang QJ, Miao TF, Zhu YY (2010) Optical switching of a metamaterial by temperature controlling. *Appl Phys Lett* 96:261908
- Messaoud TB, Landry G, Gariépy JP, Ramamoorthy B, Ashrit PV, Haché A (2008) High contrast optical switching in vanadium dioxide thin films. *Opt Commun* 281:6024–6027
- Driscoll T, Palit S, Qazilbash MM, Brehm M, Keilmann F et al (2008) Dynamic tuning of an infrared hybrid-metamaterial resonance using vanadium dioxide. *Appl Phys Lett* 93:024101
- Driscoll T, Kim HT, Chae BG, Kim BJ, Lee YW et al (2009) Memory metamaterials. *Science* 325:1518–1521
- Dai JM, Zhang JQ, Zhang WL, Grischkowsky D (2004) Terahertz time-domain spectroscopy characterization of the far-infrared absorption and index of refraction of high-resistivity, float-zone silicon. *J Opt Soc Am B* 21:1379–1386
- Jeon TI, Grischkowsky D (1997) Nature of conduction in doped silicon. *Phys Rev Lett* 78:1106–1109
- Partlow DP, Gurkovich SR, Radford KC, Denes LJ (1991) Switchable vanadium oxide films by a sol-gel process. *J Appl Phys* 70:443–452
- Ozer N (1997) Electrochemical properties of sol-gel deposited vanadium pentoxide films. *Thin Solid Films* 305:80–87
- Yuan NY, Li JH, Lin CL (2002) Valence reduction process from sol-gel V<sub>2</sub>O<sub>5</sub> to VO<sub>2</sub> thin films. *Appl Surf Sci* 191:176–180
- Guhathakurta S, Subramanian A (2007) Effect of hydrofluoric acid in oxidizing acid mixtures on the hydroxylation of silicon surface. *J Electrochem Soc* 154:136–147
- Yan JZ, Zhang Y, Huang WX, Tu MJ (2008) Effect of Mo-W Co-doping on semiconductor-metal phase transition temperature of vanadium dioxide film. *Thin Solid Films* 516:8554–8558
- Nag J, Hanlund RF Jr (2008) Synthesis of vanadium dioxide thin films and nanoparticles. *J Phys-Condens Mat* 20:264016
- Livage J, Guzman G, Beteille F, Dacardon P (1997) Optical properties of sol-gel derived vanadium oxide films. *J Sol-Gel Sci Technol* 8:857–865
- Bhushan B, Tokachichu DR, Keener MT, Lee SC (2005) Morphology and adhesion of biomolecules on silicon based surfaces. *Acta Biomater* 1:327–341
- Chan BG, Kim HT, Yun SJ, Kim BJ et al (2007) Comparative analysis of VO<sub>2</sub> thin films prepared on sapphire and SiO<sub>2</sub> substrates by the sol-gel process. *Jpn J Appl Phys* 46:738–743
- Yan JZ, Huang WX, Zhang Y, Liu XJ, Tu MJ (2008) Characterization of preferred orientated vanadium dioxide film on muscovite (001) substrate. *Phys Stat Sol* 205:2409–2412
- Jepsen PU, Fischer BM, Thoman A et al (2006) Metal-insulator phase transition in a VO<sub>2</sub> thin film observed with terahertz spectroscopy. *Phys Rev B* 74:205103
- Yang TH, Aggarwal R, Gupta A et al (2010) Semiconductor-metal transition characteristics of VO<sub>2</sub> thin films grown on c- and r-sapphire substrates. *J Appl Phys* 107:053514
- Youn DH, Kim HT, Chae BG, Hwang YJ, Lee JW, Maeng SL, Kang KY (2004) Phase and structural characterization of vanadium oxide films grown on amorphous SiO<sub>2</sub>/Si substrates. *J Vac Sci Technol A* 22:719–724